Rev. Roum. Sci. Techn.– Électrotechn. et Énerg.
Vol. **70**, *1*, pp. 47–52, Bucarest, 2025

FLICKER-FREE RESONANT DC-DC SEPIC CONVERTER WITH VALLEY-FILL FOR LED APPLICATIONS

LAKSHMI PRABA B.[1], SEYEZHAI R.[2]

Keywords: Light emitting diode (LED); Valley-fill; Single-ended primary inductor converter (SEPIC); Resonant converter; Efficiency; Ripple; Flicker; Stress.

LED lighting technology dominates the lighting market due to its long operational lifetime and excellent luminous efficiency compared to conventional light sources. Nowadays, several DC-DC SEPIC LED drivers have been presented because of the ongoing advancements in SEPIC and LED. However, the traditional SEPIC has several disadvantages: higher output current and voltage ripple, lower efficiency, and transferring all its energy with a higher capacitance value through the series capacitor. Therefore, this work deals with DC-DC SEPIC-based resonant converters with valley-fill circuits (Vfc). The proposed Vfc helps decrease the switch's current and voltage stress, increasing LED voltage and current ripple and enhancing efficiency. Therefore, a new resonant DC-DC SEPIC integrated Vfc is discussed in this work. The switch's current stress, voltage stress, LED voltage ripple, current ripple, and efficiency are evaluated, and these functional parameters are compared to the traditional SEPIC topology. As a result, a unique resonant DC-DC SEPIC integrated Vfc LED driver is developed with an efficiency of 95.6 %. MATLAB/Simulink has been used to simulate the designed circuit for the suggested topologies. A hardware prototype is created, and the results are validated.

1. INTRODUCTION

Various electrical characteristics, such as low noise and ripple, can improve power electronic converters' effectiveness and power density. To build an effective converter, switching frequency and electrical elements like power switches, diodes, inductors, and capacitors are the critical parameters. This study focuses on the converters utilized in applications for LED lighting. Various converters are offered for LED applications because of the growing need for LED technology. The focus on lighting applications has primarily focused on LED technology. These are five times more efficient than conventional lighting. As a result, they are used in various applications, including automotive, interior, and street lighting, as well as traffic signals [1,2]. Although they have many benefits, LEDs have a temperature sensitivity problem. Furthermore, because of the manufacturing process, even LEDs from the same box frequently exhibit differing values. Therefore, to guarantee a specific luminosity level, LEDs often require special trustworthy drivers to supply current with a consistent value [3–6].

The best converters for LED lighting applications are single-stage DC-DC converters [7–10]. They provide the simplest means of supplying electricity to LEDs and managing their brightness. SEPIC is implemented in this research work. The benefits of a SEPIC include its non-inverted output and ability to work in a buck or boost mode. In addition, this provides isolation between supply and load, inherent inrush current limiting at overload and startup conditions, and reduced supply current ripple associated with the DCM topology [11–13].

For further improvement in efficiency, this research work offers a SEPIC with Vfc for LED application. As a result, in an existing resonant SEPIC, the middle capacitor is replaced with the Vfc [14–16]. The significant advantages of a VFC are that it increases switching device performance, reduces the LED voltage and current ripple, and is used to reduce the current source ripple. The switch's current stress, supply current ripple, and LED current ripple are further reduced by employing a Vfc with two capacitors and three diodes [17].

Compared to several resonant converter systems, the suggested topology provides excellent efficiency throughout vast supply, LED voltages, and power levels [18–20]. Additionally, it has a minimal energy storage requirement, enabling better transient responsiveness. Unlike traditional quasi and multi-resonant converters, the proposed driver runs at a rated frequency and duty cycle and does not need a bulk inductor. These features include reduced loss and sinusoidal resonant gating and result in a more minor passive component [21,22].

Therefore, a new resonant DC-DC SEPIC integrated Vfc is developed for LED applications. The switch's voltage stress, current stress, supply side, load side voltage and current ripple, and efficiency of the resonant SEPIC with Vfc LED driver are evaluated and compared to those of the conventional SEPIC LED driver [23–25]. The resonant DC-DC SEPIC integrated with Vfc has higher performance parameters than the traditional SEPIC converter. Circuit designs for the considered topologies have been simulated with MATLAB/Simulink.

2. RESONANT SEPIC CONVERTER

The topology utilized here shares several topological similarities with the traditional SEPIC converter. Additionally, it requires minimal energy storage, enabling excellent transient responsiveness. Unlike traditional quasi and multi-resonant converters, the proposed converter runs at a fixed frequency and duty ratio and does not need a bulk inductor.

2.1 CIRCUIT OPERATION

A resonant switching element is the backbone of how a resonant converter operates. This circuit's action can be divided into two sub-intervals to be more easily understood. We can significantly simplify our model (assuming the large output filter behaves like a constant current source). Additionally, zero-voltage switching is maintained throughout a broad range of source and load voltages, and it decreases the device stress related to the converter load that occurs in many resonant systems. The circuit diagram of resonant SEPIC is displayed in Fig. 1.

This conventional driver works by coupling two subsystems. On the source side, the resonant SEPIC converter architecture operates as an inverter, while on the secondary side, a rectifier topology is used. It uses two resonant inductors: for resonant inversion mode, the

[1,2] Department of EEE, Sri Sivasubramaniya Nadar College of Engineering, Kalavakkam, Chennai, India.
E-mails: lakshmiprabab@ssn.edu.in, seyezhair@ssn.edu.in

DOI: 10.59277/RRST-EE.2025.1.8

source side inductor L_f resonates using capacitance, C_S+C_{EX}, and for rectification mode, the second inductor L_r resonates with capacitance, C_{EX2}.

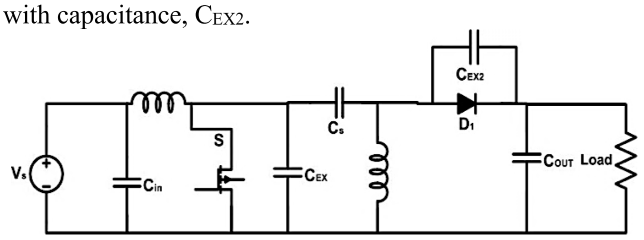

Fig.1 – Circuit diagram of the resonant SEPIC converter.

To build the rectifier, assume it is powered by an output voltage V_{out} and a sinusoidal current with I_{in} magnitude. The LC circuit tank regulates voltage and attains device zero-voltage switching (ZVS). The LC circuit operation is controlled to accomplish ZVS conditions and bidirectional operations. To achieve load voltage regulation, the circuit operation depends on frequency. The resonant inverter and resonant rectifier are two subsystems that can be connected to illustrate how this converter operates. This architecture's design procedure involves connecting the rectifier and inverter individually, then connecting them simultaneously, followed by any necessary fine-tuning to consider their non-linear interactions.

2.2 DESIGN EQUATION

MATLAB/Simulink is utilized to model and simulate the proposed modified topology. The following formulae [17–19] are used to calculate the simulation parameters. Assuming the converter operates in discontinuous current mode (DCM) and all the parameters are in perfect condition, the inductor and capacitor expression is shown below.

The conversion gain is

$$\frac{V_O}{V_{in}} = \frac{D}{1-D}, \tag{1}$$

where V_o is LED voltage, V_{in} is source voltage and D is duty ratio.

The inductor value is

$$L_f = \frac{DV_{in}}{\Delta I_0 2 f_s}, \tag{2}$$

where L_f is source side inductor, ΔI_0 is 10 to 30% of I_o and f_s is switching frequency.

The output capacitor value is

$$C_s = \frac{DI_0}{\Delta V_0 2 f_s}. \quad 3)$$

The resonant Inductor value is

$$L_r = \frac{1}{16\,\pi^2 f_r^2 C_s}, \tag{4}$$

where, L_r is resonant inductor, C_s is middle capacitor and ΔV_0 is 1 to 5% of V_0.

Resonant Capacitor value is

$$C_{EX1} = C_{EX2} = \frac{1}{16\,\pi^2 f_s^2 L_f}. \tag{5}$$

where, C_{EX1} and C_{EX2} are the resonant capacitors.

The resonant frequency f_r is defined as,

$$f_r = \frac{1}{2\pi\sqrt{L_r C_{EX2}}}. \tag{6}$$

The Vfc capacitors are

$$C_1 = C_2 = \frac{I_O D}{4\,\Delta V_O f_s}, \tag{7}$$

where, $C_1 = C_2$.

Equations (1) to (7) are the design equations for resonant SEPIC with and without valley-fill circuit LED Drivers.

2.3 SIMULATION RESULTS

The design variables are determined by using the formulas depicted in subsection 2.2, and the specifications are displayed in Table 1.

Table 1

Design variables.

Design Variables	Values
Supply voltage	12 V
Operating frequency	30 kHz
Duty cycle	0.67
Capacitance (*Cs* and *Cin*)	297 pF
Inductor (L_1)	2.412 mH
Filter capacitor	500 µF
Resonant capacitor	397 pF
Resonant Inductor	60 µH
Resonant Frequency	1 MHz
LED	24 V, 0.42 A

The simulation waveforms for the resonant SEPIC LED driver using Matlab/Simulink are displayed below using the design parameters that are depicted in Table 1.

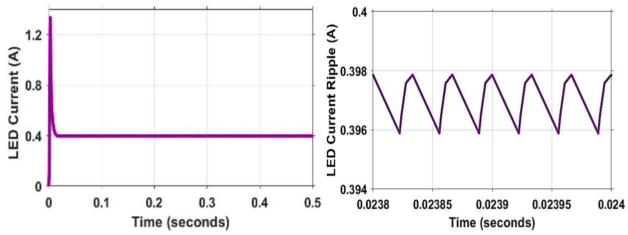

Fig. 2 – Load current and current ripple waveform for resonant SEPIC converter.

From Fig. 2, the obtained LED current value of the resonant SEPIC converter is around 0.4 A, and the ripple current value is around 1.06 %.

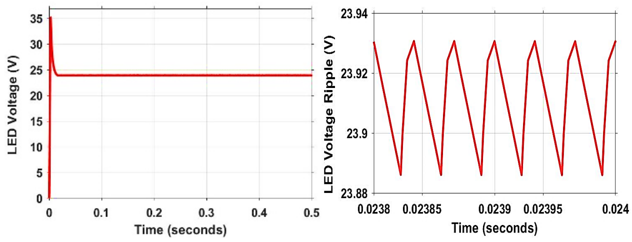

Fig. 3 – Load voltage and ripple voltage waveform for resonant SEPIC converter.

From Fig.3, the attained LED voltage value of the resonant SEPIC LED driver is around 24 V, and the ripple voltage value is around 0.212 %.

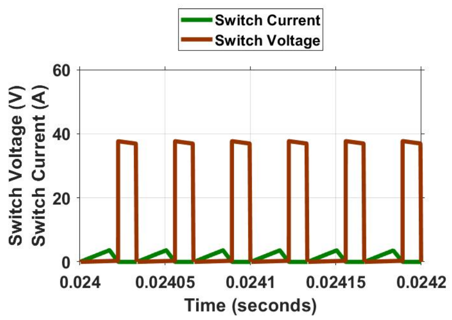

Fig. 4 – ZVS waveform for resonant SEPIC LED driver.

From Fig. 4, the obtained switch current and voltage stress in resonant SEPIC LED driver are about 3.6 A and 39.6 V, respectively.

3. PROPOSED RESONANT SEPIC CONVERTER WITH VFC LED DRIVER

This research paper comprehensively deals with the resonant SEPIC integrated with a based LED driver. This VFC consists of three diodes and two capacitors, and it offers higher efficiency over extensive supply and LED voltage ranges and power levels; in contrast to several resonant converter systems, reduced current and voltage ripple, current stress across the semiconductor device is also reduced by employing this Vfc.

3.1 CIRCUIT DESIGNING METHODS

The circuit diagram of the resonant SEPIC integrated Vfc driver is depicted in Fig. 5. Then, the design methods of the resonant SEPIC with Vfc LED driver are divided into three, which are discussed below. Based on the assumption,

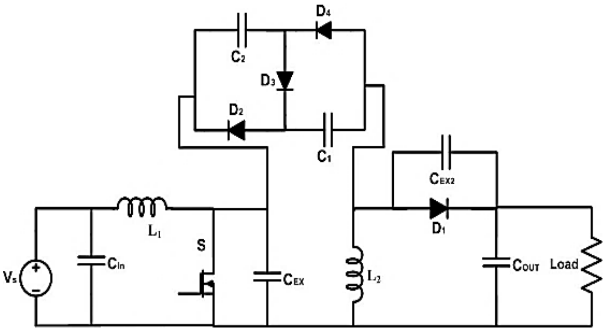

Fig. 5 – Circuit diagram of the resonant SEPIC LED driver with Vfc.

Rectification stage: This stage is designed as a current-driven rectifier, as shown in Fig 6,a. Based on the assumption, the fundamental component is expected to give the most output power when applying a sinusoidal supply current with an amplitude of Iin to the rectifier stage. The amplitude of Iin must be taken into consideration when tuning.

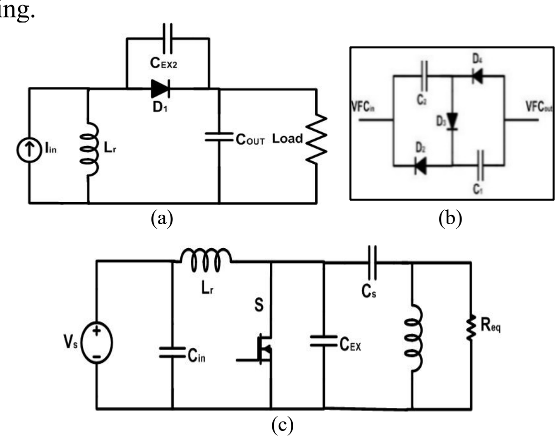

Fig. 6 – (a) Rectification Stage (b) Valley fill stage (c) Inversion stage

Vfc stage: The middle capacitor in that resonant SEPIC converter is interchanged into the Vfc to create a high gain, reduced current ripple, supply current ripple, reduced voltage ripple, and decreased voltage and current stress across the power MOSFET. Two capacitors and three diodes comprise this Vfc.

The capacitor Cs is split into two Vfc capacitors named C_1 and C_2. The diodes D_2 and D_4 are used to discharge the capacitors C_1 and C_2 in parallel after charging them in series. To stop C_2 from discharging through C_1, diode D_3 is placed. Simulation with a more significant load or experimental testing makes this effect easy to verify. This assumes that a lesser load will require less output current, preventing the charges on C_1 and C_2 from being considerably depleted quickly and causing the charging spike to be narrower than its counterpart for a heavier load. This Vfc is used to reduce LED current and LED voltage ripple.

Inversion stage: The inverter network is shown in Fig 6.c. The first step in inverter tuning is choosing the right components. The equivalent impedance R_{eq} is to model this rectification stage. The primary guidelines for designing the inversion are to achieve ZVS for the switch and an improved power conversion.

3.2 SIMULATION RESULTS

The resonant SEPIC integrated Vfc LED driver specifications for the components are designed using the designs eq. (1) to (7), and the design variables are displayed in Table 2.

Table 2

Design Specifications.

Design Variables	Values
Source voltage	12 V
Operating frequency	30 kHz
Duty cycle	0.67
Capacitance (C_s and C_{in})	297 pF
Inductor (L_1)	2.412 mH
Filter capacitor	100 µF
Vfc capacitors	13 µF
Resonant capacitor	397 pF
Resonant Inductor	60 µH
Resonant Frequency	1 MHz
LED	24 V, 0.42 A

The simulation waveforms for the resonant SEPIC integrated Vfc LED driver using MATLAB/Simulink are displayed below by the simulation parameters listed in Table 2.

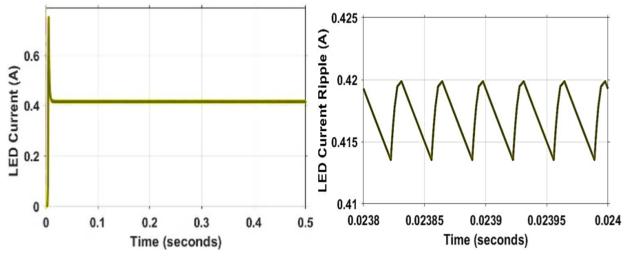

Fig. 7 – LED current and ripple current waveform of the resonant SEPIC Vfc LED driver.

From Fig.7, the attained LED current value and the ripple current value of resonant SEPIC Vfc LED driver are around 0.42 A and 0.98 %, respectively.

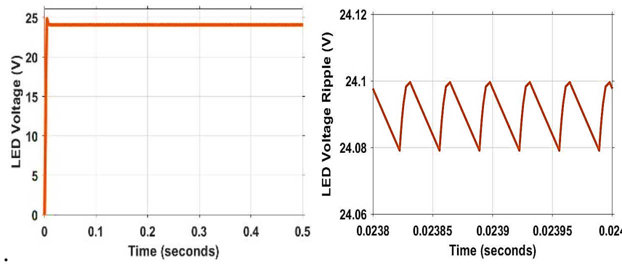

Fig. 8 – LED voltage, ripple of the resonant SEPIC with Vfc LED driver.

From Fig.8, the obtained LED voltage and the ripple voltage values of resonant SEPIC Vfc LED driver are around 24.1 V, and 0.084 %, respectively.

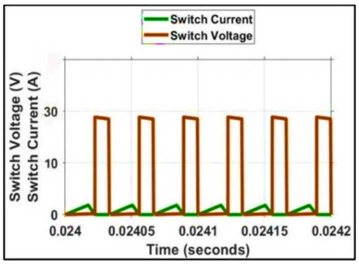

Fig. 9 – ZVS waveform of the resonant SEPIC Vfc LED driver.

From Fig. 9, the obtained switch current and voltage stress in the proposed SEPIC Vfc converter are about 2.2 A and 28 V, respectively.

4. COMPARISON WITH OTHER TOPOLOGIES

The performance metrics of the proposed resonant SEPIC Vfc converter are compared with the following three topologies. These are conventional SEPIC LED drivers, conventional SEPIC LED with Vfc, and resonant SEPIC Vfc LED drivers.

Table 3

Comparison of performance parameters.

Topology/ Parameters	V_o (V)	I_o (A)	V_o ripple (%)	I_o ripple (%)	Input current (A)	Input current ripple (%)	Efficiency (%)
Con-SEPIC	24.5	0.42	1.59	0.24	0.85	15.7	88
Con-SEPIC with Vfc	24.2	0.43	0.93	0.13	0.86	12.7	91
Res-SEPIC	23.9	0.4	1.05	0.212	0.82	14.8	92.5
Res-SEPIC with Vfc	24.1	0.42	0.98	0.084	0.85	9.88	93.7

Table 4

Stress in the switch and output diode.

Topology/ Parameters	Switch current stress (A)	Switch stress voltage (V)	D_1 stress current (A)	D_1 stress voltage (V)
Con-SEPIC	5.9	46	5.7	40
Con-SEPIC with Vfc	5.6	37	4	38
Res- SEPIC	3.6	39.6	2.7	31.5
Res-SEPIC with Vfc	2.2	28	1.3	25

The conventional SEPIC and SEPIC with Vfc performance parameters and attributes are compared to the proposed resonant SEPIC with Vfc. The resonant SEPIC with Vfc and the resonant SEPIC without Vfc are quantitatively analyzed in Tables 3 and 4. The topologies mentioned above are simulated with a 12 V input voltage, and the outcomes are evaluated for more precise comparisons. The comparison shows that the recommended resonant SEPIC with Vfc LED driver offers superior performance in LED voltage ripple, current ripple, efficiency, and stress placed on the output diodes and semiconductor switches. Due to reduced LED current ripple, the flickering is also lesser.

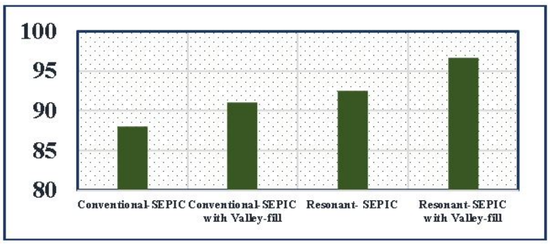

Fig. 10 – Efficiency comparison.

Since efficiency impacts heat production and total energy consumption, it is crucial for DC-DC LED drivers. High-efficiency drivers reduce power loss and improve the sustainability of LED lighting systems by minimizing energy losses during the conversion process. From Fig. 10, the efficiency of the proposed resonant SEPIC with Vfc is higher than that of the other topologies.

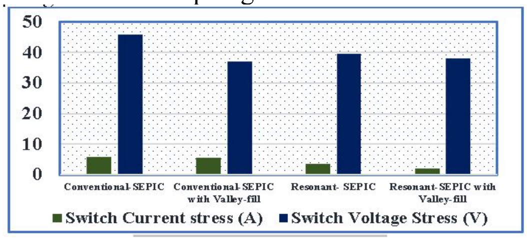

Fig. 11 – Switch stress comparison.

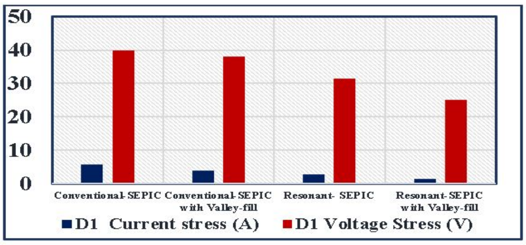

Fig. 12 – Diode stress comparison.

Excessive current stress can result in overheating and failure, reducing the driver's overall efficiency and lifespan, while high voltage stress can induce breakdown. It is evident from Figs. 11 and 12 that the resonant SEPIC with valley fill LED driver has the least voltage and current stress in both the switch and output diode.

5. EXPERIMENTAL SETUP

An experimental model is implemented, and the outcomes are reported to demonstrate the simulation outcomes. A prototype of a resonant DC-DC SEPIC with a Vfc LED driver is developed using MOSFET, gate drivers, and optocoupler circuits. The resonant SEPIC with the Vfc LED driver output and its performance metrics are determined and validated. The experimental setup of the proposed driver is built based on the design parameters, the same as the simulation displayed in Table 2. The hardware results of the suggested LED driver are recorded using a scope coder DL850 (Yokogawa) for a rated power of 10 W.

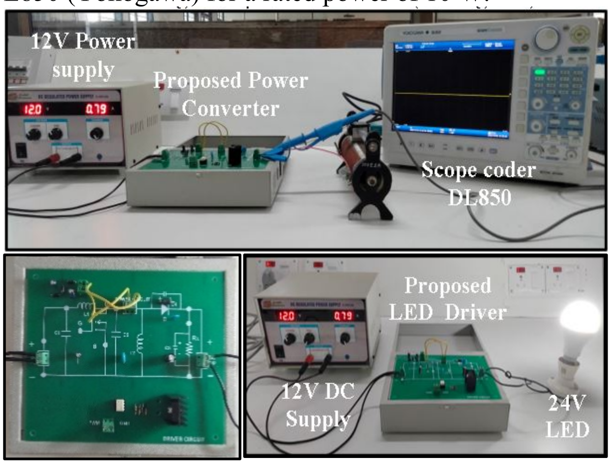

Fig. 13 – Experimental setup of resonant SEPIC with Vfc LED driver.

The resonant SEPIC can power a 10 W LED with a Vfc LED driver with a voltage range of 24 V. To power the LED, 12 V of voltage and a current of 0.42 A is required. The experimental setup for the projected converter and the relevant waveforms of the proposed resonant SEPIC with Vfc LED driver are displayed in Figs. 14-16.

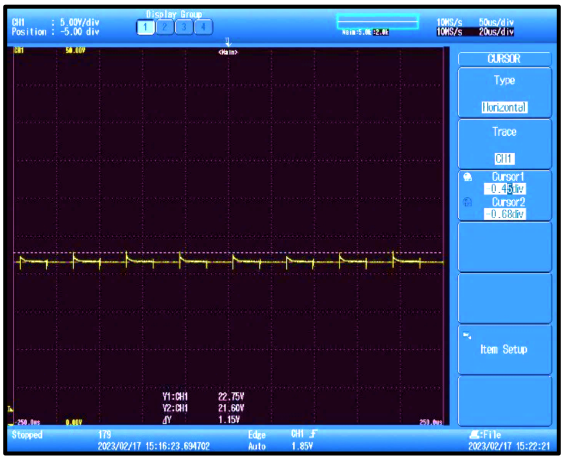

Fig. 14 – LED voltage waveform of resonant SEPIC with Vfc.

From Fig.14, the LED voltage for resonant SEPIC with Vfc LED driver is around 22.75 V with a ripple of 1.15 V.

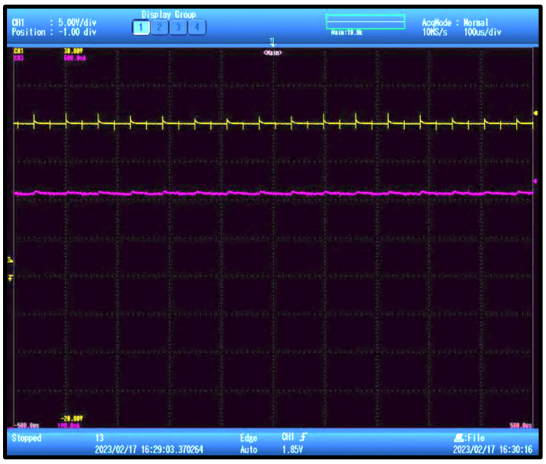

Fig. 15 – LED current waveform of resonant SEPIC with Vfc LED driver.

From Fig.15, the LED current of resonant SEPIC with Vfc LED driver is around 0.42 A with a ripple of 15 mA.

Fig. 16 – Voltage and current stress across the switch in resonant SEPIC with Vfc LED driver.

From Fig.16, the stress voltage and current across the switch in the proposed LED driver are about 23 V and 4.2 A. Table 5 displays an extensive comparison of the experimental and simulated results.

Table 5

Comparison of simulated and experimental results.

Parameters	Simulation values	Experimentation values
Switch current and voltage	28V and 2.2A	23V and 4.2A
LED voltage (V_{LED})	23.8V	22.75V
V_{LED} ripple	0.084%	1.15V
LED current (I_{LED})	0.41A	0.42A
I_{LED} ripple	10.8mA	15mA

From Table 5, the proposed resonant Vfc-based converter ripple is within the admissible limits as per IEEE Std 1789-2015, *i.e.*, the proposed LED driver's ripple current is 15 mA, and the voltage ripple is 1.15 V.

6. CONCLUSION

This work presents a proposed resonant DC/DC SEPIC LED driver integrated with a Vfc circuit for LED driver applications.

Compared to traditional DC/DC SEPIC LED drivers, this design significantly reduces voltage and current ripple, enhances efficiency, and minimizes stress on the switching devices. A 10 W prototype of the proposed driver operates at 30 kHz, providing a LED voltage of 22.75 V with a ripple of 1.75 V, a current of 0.42A with a ripple of 15 mA, and stress across the switch of 23V and 4.2 A.

The system achieves an overall efficiency of 93.7 %. Furthermore, the resonant DC/DC SEPIC with the Vfc circuit is highly suitable for ripple-free LED applications.

Future research could focus on reliability predictions and alternative ripple cancellation algorithms for the proposed topology.

CREDIT AUTHORSHIP CONTRIBUTION STATEMENT

L. Praba B.: Investigation, visualization, writing—original draft, software, validation.

R. Seyezhai: Project administration, supervision, resources.

Received on 19 January 2024

REFERENCES

1. D.R. Corrêa, A. Silva de Morais, F.L. Tofoli, *Non-isolated quadratic SEPIC converter without electrolytic capacitors for LED driver applications*, 15th Brazilian Power Electronics and 5th IEEE Southern Power Electronics Conference, pp. 1–7 (2019).
2. Y. Wang, J.M. Alonso, X. Ruan, *A review of LED drivers and related technologies*, IEEE Trans. Ind. Electron., **64**, *7*, pp. 5754–5765 (2017).
3. C.C. Raicu, G.C. Seritan, B. Enache, *48 V network adoption for automotive lighting systems*, Rev. Roum. Sci. Techn. –Électrotechn. Et Énerg, **66**, *4*, pp. 231–236 (2021).
4. G. Vacheva, N. Hinov, B. Gilev, *Computer investigation of SEPIC DC-DC converter for LED lighting applications*, Second Balkan Junior Conference on Lighting, pp. 1–4 (2019).
5. J. Singh, P. Mahajan, R. Garg, *Design & implementation of solar fed intensity-controlled streetlight*, 2nd IEEE International Conference on Power Electronics, Intelligent Control, and Energy Systems, pp. 671–676 (2018).
6. S. Ahmad, N.M.L. Tan, M.Z. Baharuddin, G. Buticchi, *A high-performance isolated SEPIC converter for non-electrolytic LED lighting*, in IEEE Access, **9**, pp. 149894–149905 (2021).
7. V. Naithani, A.N. Tiwari, S. Dobhal, *Simulation of sepic converter fed LED's*, International Journal of Engineering Science and Technology, **4**, *3*, pp. 1015–1020 (2012).

8. S. Singh, B. Singh, *Single-phase SEPIC based PFC converter for PMBLDC motor drive in air-conditioning system*, Asian Power Electronics Journal, **4**, *1*, pp. 16–21 (2010).
9. D.S.L. Simonetti, J. Sebastian, J. Uceda, *The discontinuous conduction mode SEPIC and CUK power factor pre-regulators: analysis and design*, in IEEE Trans. on Industrial Electronics, **44**, *5*, pp. 630–637 (1997).
10. A. Sureshkumar, R. Gunabalan, *Design and implementation of single switch control DC-DC converter with wide input variation in automotive LED lighting*, Int. Trans. Elect. Energy Syst., **31**, *4* (2021).
11. M. Dalla Vecchia, G. Van den Broeck, S. Ravyts, J. Tant, J. Driesen, *A family of DC–DC converters with high step-down voltage capability based on the valley-fill switched capacitor principle*, in IEEE Transactions on Industrial Electronics, **68**, *7*, pp. 5810–5820 (2021).
12. S. Hariprasath., R. Balamurugan, A *valley-fill SEPIC-derived power factor correction topology for led lighting applications using one cycle control technique*, International Conference on Computer Communication and Informatics, IEEE (2013).
13. H. Ma, C. Zheng, W. Yu, J. -S. Lai, *Bridgeless electrolytic capacitor-less valley fill AC/DC converter for twin-bus type LED lighting applications*, 1st International Future Energy Electronics Conference, pp. 304–310 (2013).
14. D. Dah, C. Lu, *Analysis of an AC-DC valley-fill power factor corrector*, ECTI Transactions on Electrical Eng., Electronics, and Communications, **5**, *2* (2007).
15. N. Molavi, H. Farzanehfard, *Load-independent hybrid resonant converter for automotive LED driver applications*, in IEEE Trans. on Power Electronics, **377**, pp. 8199–8206 (2022).
16. Z. Zhang, J. Lin, Y. Zhou, X. Ren, *Analysis and decoupling design of a 30 MHz resonant SEPIC converter*, in IEEE Transactions on Power Electronics, **31**, *6*, pp. 4536–4548 (2016).
17. J. Hu, A. D. Sagneri, J.M. Rivas, Y. Han, S.M. Davis, D.J. Perreault, *High-frequency resonant SEPIC converter with wide input and output voltage ranges*, in IEEE Transactions on Power Electronics, **27**, *1*, pp. 189–200 (2012).
18. R. Erickson, D. Maksimović, *Fundamentals of Power Electronics*, Norwell, MA, Kluwer (2000).
19. J. Zhao, Y. Han, *A novel switched capacitor based partial power architecture for a 20 MHz resonant SEPIC*, IEEE Energy Conversion Congress and Exposition, pp. 1442–1449 (2015).
20. K.T. Chau, M. Wong, *Valley-fill technique for reducing voltage ripple in DC-DC converters*, IEEE Trans. on Power Electronics, **22**, *5*, 1881–1889 (2007).
21. H.T.H. Van, T.L. Van, T.M.N. Thi, M.Q. Duong, G.N. Sava, *Improving the output of dc-dc converter by phase shift full bridge applied to renewable energy*, Rev. Roum. Sci. Techn.–Électrotechn. Et Énerg., **66**, *3*, pp.175–180 (2021).
22. S. Gao, Y. Wang, Y. Liu, Y. Guan, D. Xu, *A novel DCM soft-switched SEPIC-based high-frequency converter with high step-up capacity*, in IEEE Transactions on Power Electronics, **35**, *10*, pp. 10444–10454 (2020).
23. S. Mukherjee, V. Yousefzadeh, A. Sepahvand, M. Doshi, D. Maksimović, *High-frequency wide range resonant converter operating as an automotive LED driver*, IEEE Trans. Emerg. Sel. Topics Power Electron., **9**, *5*, pp. 5781–5794 (2020).
24. F.I. Kravetz, R. Gules, *Soft-switching high static gain modified SEPIC converter*, in IEEE Journal of Emerging and Selected Topics in Power Electronics, **9**, *6*, pp. 6739-6747 (2021).
25. S. Makkapati, S. Ramalingam, *Lifetime prediction of LED driver using Bayesian belief network*, Rev. Roum. Sci. Techn. –Électrotechn. Et Énerg, **68**, *4*, pp. 351–356 (2023).